Transfer mechanism for 3α in heavy ion scattering

Linhua Xia and Guozhu He

Theoretical Physics Division of Nankai Institute for Mathematics, Nankai University, Tianjin, China

(Received 20 October 1986)

A molecular orbital theory for the 3α transfer process has been formulated and applied to the $^{16}O + ^{28}Si$ scattering case. The α transfer mechanism has already been applied successfully in the interpretation of the anomalous large angle scattering between $4N$ nuclei. It would be worthwhile to test whether the alpha transfer mechanism can also explain the nonstatistical intermediate structure of the excitation function often found in $4N$ nuclei scattering. The excitation function at $180°$ is known to be much more sensitive to the details of the optical potential than are the fits to the angular distribution. Both the experimental data of the excitation function at $180°$ in the energy region from 14 to 52 MeV and all thirteen differential cross sections in the energy region $18.67-34.80$ MeV can be fitted well simultaneously with a common set of parameters.

I. INTRODUCTION

$^{16}O + ^{28}Si$ is one of the most thoroughly investigated scattering systems.[4-21] Its excitation function has been accurately measured in a wide energy region from 14 to 52 MeV at the backward angle region, and shows a complicated structure, as shown in Fig. 1. There exist many peaks with widths on the order of $1-3$ MeV. The lifetimes of these peaks are much too short to form a compound nucleus and have nearly the same order of magnitude as that of direct potential scattering of two nuclei passing through each other. This might indicate that certain nonstatistical structures could be formed momentarily with weak binding potential during the colliding process.

Scattering differential cross sections in the whole angle region are available in 13 different energies from 18.67 to 34.80 MeV, as shown in Fig. 2. The rising oscillatory structure observed in the large angle region changes systematically with increasing incident energy. This set of experimental curves furnishes an ideal case with which to test different models proposed for interpreting these anomalous phenomena.

Many theoretical models have been put forward in an attempt to explain these anomalous phenomena, the rising oscillatory structure in the large angle region (ALAS) and the intermediate nonstatistical structure (INS) of $^{16}O + ^{28}Si$.[9-21] Some modified optical potentials with surface correction or with additional parity dependent terms were proposed to fit these experimental data. Kobos and co-workers[12,13] found that two optical potentials were needed. One describes the data at eleven energies between 18 and 29 MeV and the other for two energies, 31.6 and 34.8 MeV.

A number of model independent expressions have also been sought for the potential of this scattering system.[7,12-18] Good fits were obtained with the measured angular distribution. However, when no constraints were placed on them, the resulting real potentials were not unique. A short range repulsive term has been introduced into the real part of the optical potential to explain the large angle scattering data at higher energies, in order to deal with the strong resistance and the dynamical effect, to prevent interpenetration as the two nuclei overlap each other.[19-21]

Besides these phenomenological optical potential models, another possible approach is consideration of the α-transfer contribution in the scattering. It has been successful in the interpretation of ALAS for certain scattering cases between $4N$ nuclei, by considering one and two alpha particle transfer in the scattering processes, such as $^{16}O + ^{20}Ne$, $^{12}C + ^{20}Ne$, and $^{16}O + ^{24}Mg$.[1-3]

For this $^{16}O + ^{28}Si$ elastic scattering case, in addition to the direct potential scattering, one could expect two kinds of transfer processes to occur: a ^{12}C cluster transfer and the transfer of three alpha particles from ^{28}Si to ^{16}O. As it is well-known that there is substantial possibility for an α particle to be formed at the surface of a nucleus, during the scattering process of ^{16}O with ^{28}Si three alpha particles may be formed. These α particles will interact with the nuclear cores and temporary molecular orbits may exist. Eventually, these α particles will be shared by the cores and, as a result, they may be transferred.

Since the two nuclear cores are identical in this case, one cannot distinguish experimentally the direct optical potential scattering from the scattering with three alpha particles transferred. In the backward angle region one may detect both the ^{16}O scattered backward by the optical potential and also the target core ^{16}O after ^{28}Si transferred three α particles to the incident nucleus. This may be the reason why there is a rise of the cross section when observing ^{16}O in the backward angle region. By adding the contribution of these two kinds of processes, the ALAS may be explained rather naturally. The interference of the direct and transfer waves gives rise to the oscillatory structure of the angular distribution at large angles. It is expected that the formation of molecular orbits in the combined scattering system results in the intermediate
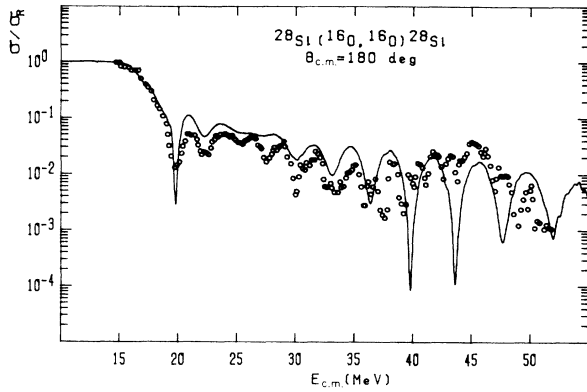
FIG. 1. Excitation function for $^{16}O + {}^{28}Si$ in comparison with a 3α transfer molecular orbital model prediction.

nonstatistical structure of the excitation function.

Since the α particle has the largest binding energy, it has the most probability of being formed at the surface and in the overlapping region of the colliding nuclei. Furthermore, since the correlation between α particles is weak, the possibility of the formation and transfer of a ^{12}C cluster in the scattering process could be small. The contribution of ^{12}C transfer in the scattering is then neglected.

A molecular orbital theory has been formulated for the 3α transfer mechanism in the scattering process, with the assumption that all the α particles stay at the ground states. Taking the indistinguishability of both the identical nuclear cores and the α particles into consideration, one finds that there exists a set of four possible molecular orbits. The total potential energy for the scattering system is now different for different orbits. In addition to the ordinary optical potential for the direct scattering, for each molecular orbit a particular exchange potential appears. Due to the symmetry properties, these exchange potentials are quite different from each other. Some are repulsive and some are attractive in the overlapping region.

The total potential energy of the system which now includes the optical, Coulomb, and exchange potentials has been plotted numerically. In many cases it actually gives the Morse-type potential with a shape which has a shallow attractive well in the overlapping region needed to form molecular orbits and which becomes repulsive for closer separation of the two cores. It is found that the 14 experimental curves of both excitation functions and angular distributions available can be reproduced fairly well simultaneously with one set of parameters chosen in the calculation.

II. MOLECULAR ORBITAL (LCNO) THEORY FOR 3α TRANSFER MECHANISM

Consider a colliding system composed of two identical nuclear cores C_I and C_{II}, with three α particles revolving about them. Since the correlation between the α particles is weak, the residual interaction between them is neglected

and the Hamiltonian of the system can then be written as

$$H = T_{I,II} + V_{I,II} + h ,$$
$$h = \sum_i h_i \quad \text{and} \quad h_i = t^i + v_I^i + v_{II}^i, \quad i = 1,2,3 \tag{1}$$

where h_i is the Hamiltonian for the ith α particle, and v_I^i and v_{II}^i are its interaction with cores I and II, respectively.

Let the wave function of a valence particle be $\Phi_{p_i}(I,II,i)$, which satisfies

$$h_i \Phi_{p_i}(I,II,i) = \epsilon_{p_i} \Phi_{p_i}(I,II,i) . \tag{2}$$

Under the two-state approximation the valence particle α can stay in the ground state binding to either core I or II. Its wave function is then expressed by the expansion of these ground states of two identical cores, ϕ_I and ϕ_{II}. ϕ_j satisfies $(t + V_j)\phi_j = \epsilon\phi_j$, $j = I,II$,

$$\Phi_{p_i} = [2(1 + p_i\delta)]^{-1/2}[\phi_I(i) + p_i\phi_{II}(i)] . \tag{3}$$

This expression ensures the exchange symmetry property of the two identical cores, $\delta = \langle \phi_I(i) | \phi_{II}(i) \rangle$.

Neglecting the recoil of the nuclear cores, one gets

$$\epsilon_{p_i} = \epsilon + (K + p_i J)/(1 + p_i\delta) , \tag{4}$$

where $\epsilon = \langle \phi_I | t + v_I | \phi_I \rangle$ is the interior binding energy, $K = \langle \phi_I | v_{II} | \phi_I \rangle$ the direct integral, and $J = \langle \phi_I | v_{II} | \phi_{II} \rangle$ the exchange potential. When the correlation between the valence particles is neglected, the total molecular orbital state function can be written as

$$\Phi_{p_1 p_2 p_3} = \Phi_{p_1} \Phi_{p_2} \Phi_{p_3}$$
$$= \prod_{i=1}^{3} [2(1 + p_i\delta)]^{-1/2}[\phi_I(i) + p_i\phi_{II}(i)] . \tag{5}$$

It satisfies

$$\langle \Phi_{p_1 p_2 p_3} | \Phi_{p_1' p_2' p_3'} \rangle = \delta_{p_1 p_1'} \delta_{p_2 p_2'} \delta_{p_3 p_3'} ,$$

and its energy is

$$\epsilon_{p_1 p_2 p_3} = 3\epsilon + \sum_{i=1}^{3} (K + p_i J)/(1 + p_i\delta) . \tag{6}$$

Since in Eq. (5) p_i can be ± 1, in the expansion there are all together eight independent molecular states. Furthermore, if one also takes the identical symmetry property of the valence particles into consideration, these eight states have to be combined to get a complete orthonormal set of four totally symmetrical wave functions:

$$\Phi_1 = \Phi_{---} ,$$
$$\Phi_2 = \Phi_{+++} ,$$
$$\Phi_3 = 3^{-1/2}(\Phi_{-++} + \Phi_{+-+} + \Phi_{++-}) , \tag{7}$$
$$\Phi_4 = 3^{-1/2}(\Phi_{+--} + \Phi_{-+-} + \Phi_{--+}) .$$

These form the four possible molecular orbital states for the system considered, with two identical spinless nuclear cores and three identical spinless valence particles. Φ_1 and Φ_3 correspond to odd partial waves, while Φ_2 and Φ_4 correspond to even partial waves. Now expand the wave
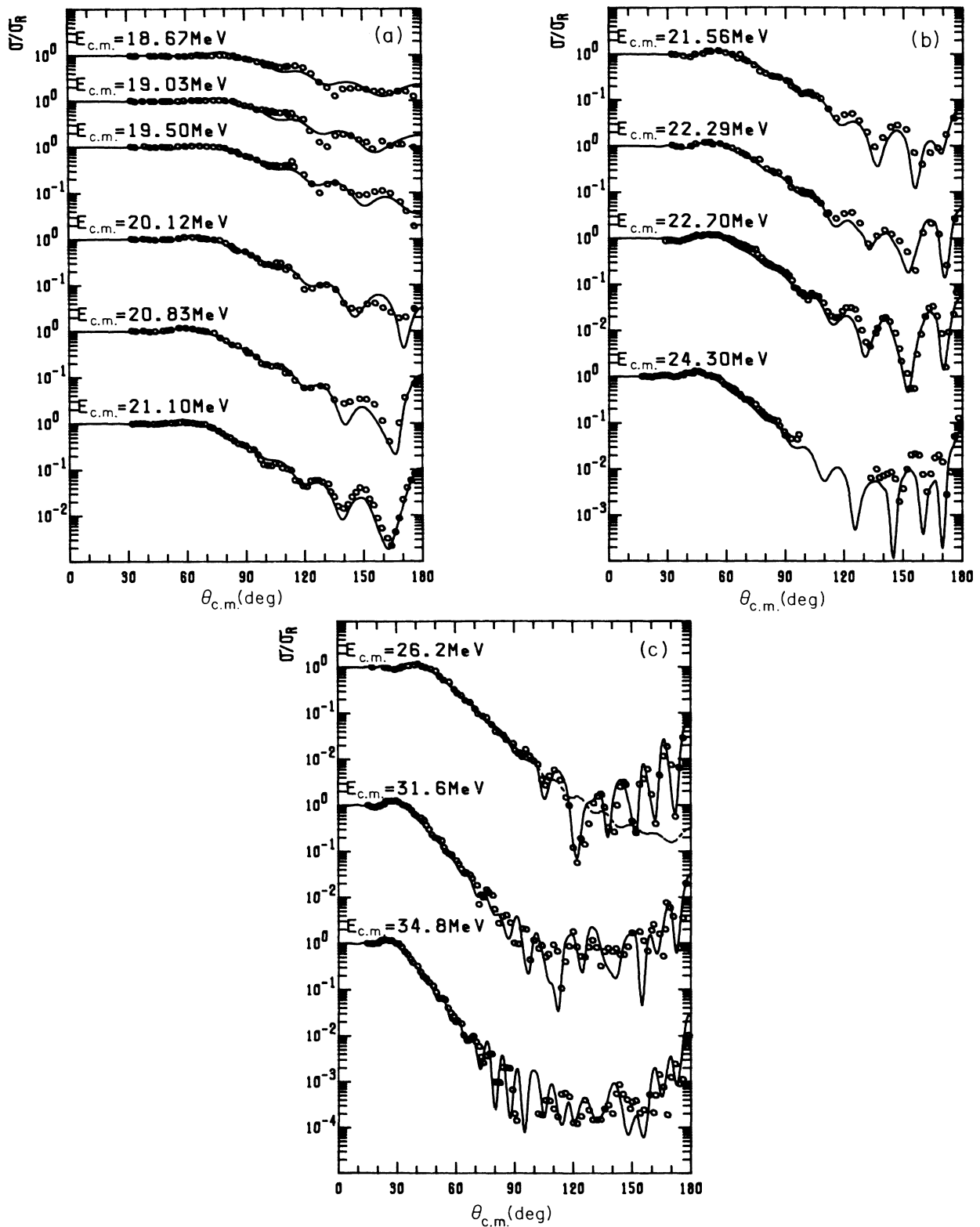
FIG. 2. (a) Differential cross section for $^{16}O + {}^{28}Si$ in comparison with a 3α transfer molecular orbital model prediction. $E=18.67-21.10$ MeV. (b) Differential cross section for $^{16}O + {}^{28}Si$ in comparison with a 3α transfer molecular orbital model prediction. $E=21.56-24.30$ MeV. (c) Differential cross section for $^{16}O + {}^{28}Si$ in comparison with a 3α transfer molecular orbital model prediction. $E=26.20-34.80$ MeV. In the $E=26.20$ MeV case a dashed curve is drawn to show the calculation with the exchange potential deliberately deleted. It shows that the exchange potential appears to play a major role for the rise in the backward angle region.

function of the system in terms of these possible molecular states,

$$\Psi = \sum_{\mu=1}^{4} C_\mu F_\mu(\text{I},\text{II}) \Phi_\mu(\text{I},\text{II},123) \;, \tag{8}$$

where $F_\mu(\text{I},\text{II})$ represents the relative motion of the nuclear cores. As one knows,

$$\Phi_\mu(\text{II},\text{I},123) = (-1)^\mu \Phi_\mu(\text{I},\text{II},123) \;.$$

F_μ should have the following symmetry property against exchange of nuclear cores:

$$F_\mu(\text{II},\text{I}) = (-1)^\mu F_\mu(\text{I},\text{II}) \;.$$

For $(-1)^\mu = 1$, F_μ contains only even partial waves, while for $(-1)^\mu = -1$, F_μ has odd partial waves. The molecular states satisfy

$$\langle \Phi_\mu \mid \Phi_\nu \rangle = \delta_{\mu\nu} \quad \text{and} \quad \langle \Phi_\mu \mid h \mid \Phi_\nu \rangle = \epsilon_\mu \delta_{\mu\nu} \;.$$

From Eq. (6), one gets

$$\begin{aligned}
\epsilon_1 &= 3[\epsilon + (K - J)/(1-\delta)] \;, \\
\epsilon_2 &= 3[\epsilon + (K + J)/(1-\delta)] \;, \\
\epsilon_3 &= 3\epsilon + 2(K + J)/(1+\delta) + (K - J)/(1-\delta) \;, \\
\epsilon_4 &= 3\epsilon + 2(K - J)/(1-\delta) + (K + J)/(1+\delta) \;.
\end{aligned} \tag{9}$$

Expand Eq. (5) and define

$$\Phi_{\text{ion}}^{\pm} = [2(1\pm\delta^3)]^{-1/2}[\phi_{\text{I}}(1)\phi_{\text{I}}(2)\phi_{\text{I}}(3) \pm \phi_{\text{II}}(1)\phi_{\text{II}}(2)\phi_{\text{II}}(3)] \;, \tag{10a}$$

$$\begin{aligned}
\Phi_{\text{mix}}^{\pm} = [6(1\pm\delta)(1\pm\delta+\delta^2)]^{-1/2}\{[\phi_{\text{II}}(1)\phi_{\text{I}}(2)\phi_{\text{I}}(3) \pm \phi_{\text{I}}(1)\phi_{\text{II}}(2)\phi_{\text{II}}(3)] \\
+ [\phi_{\text{I}}(1)\phi_{\text{II}}(2)\phi_{\text{I}}(3) \pm \phi_{\text{II}}(1)\phi_{\text{I}}(2)\phi_{\text{II}}(3)] + [\phi_{\text{I}}(1)\phi_{\text{I}}(2)\phi_{\text{II}}(3) \pm \phi_{\text{II}}(1)\phi_{\text{II}}(2)\phi_{\text{I}}(3)]\} \;. \tag{10b}
\end{aligned}$$

The first term in Eq. (10a) expresses the state with three valence particles bound on a core. It is called an ionic state. The other three terms in Eq. (10b) express states with two valence particles bound on one nuclear core and the third particle bound on another core, and are called mixed states. Φ_μ may be then written in terms of these two kinds of states:

$$\begin{aligned}
\Phi_1 &= [2(1-\delta)]^{-1/2}[(1+\delta+\delta^2)^{1/2}\Phi_{\text{ion}}^{-} \\
&\quad - 3^{1/2}(1-\delta+\delta^2)^{1/2}\Phi_{\text{mix}}^{-}] \;, \\
\Phi_2 &= [2(1+\delta)]^{-1/2}[(1-\delta+\delta^2)^{1/2}\Phi_{\text{ion}}^{+} \\
&\quad + 3^{1/2}(1+\delta+\delta^2)^{1/2}\Phi_{\text{mix}}^{+}] \;, \\
\Phi_3 &= [2(1+\delta)]^{-1/2}[3^{1/2}(1+\delta+\delta^2)^{1/2}\Phi_{\text{ion}}^{-} \\
&\quad + (1-\delta+\delta^2)^{1/2}\Phi_{\text{mix}}^{-}] \;, \\
\Phi_4 &= [2(1-\delta)]^{-1/2}[3^{1/2}(1-\delta+\delta^2)^{1/2}\Phi_{\text{ion}}^{+} \\
&\quad - (1+\delta+\delta^2)^{1/2}\Phi_{\text{mix}}^{+}] \;.
\end{aligned} \tag{11}$$

Now let us solve the integral

$$\langle \Phi_\mu \mid E - H \mid \Psi \rangle = 0 \;.$$

Under the two-state approximation, one obtains the wave equation of the relative motion of the cores for different molecular states,

$$(E - T_{\text{I},\text{II}} - V_{\text{I},\text{II}} - \epsilon_\mu)F_\mu = 0, \quad \mu = 1,2,3,4 \;. \tag{12}$$

The combinations of the scattering amplitudes of outgoing F_μ give the differential cross sections.

One can see from Eq. (12) that, in addition to the optical potential $V_{\text{I},\text{II}}$ which causes the direct scattering, another potential or energy term, ϵ_μ, which may be called the molecular orbital potential, appears from the contribu-

tion of forming molecular orbits and exchanging valence particles. E in Eq. (12) is the center of mass energy of the system.

The ϵ_μ are different for four different molecular states, as shown in Eq. (9). Different partial waves will encounter different potentials, either attractive or repulsive. It is this molecular orbital potential which causes the rising oscillatory structure in the large angle region and gives the intermediate structure in the excitation function.

The outgoing wave function of the colliding system can be found easily:

$$\Psi_{\text{out}} \to \tfrac{1}{4}[(f_1 + 3f_3)\Phi_{\text{ion}}^{-} + (f_2 + 3f_4)\Phi_{\text{ion}}^{+}]e^{ikR}/R$$
$$- \left| \frac{\sqrt{3}}{4} \right| [(f_1 - f_3)\Phi_{\text{mix}}^{-} - (f_2 - f_4)\Phi_{\text{mix}}^{+}]e^{ikR}/R \;,$$

where the f_i are the scattering amplitudes of the outgoing waves from different molecular states. The differential cross sections for the two processes are then expressed in terms of the four scattering amplitudes:

$$\left. \frac{d\sigma}{d\Omega} \right|_{\text{ion}} = \tfrac{1}{16} \mid f_1 + f_2 + 3f_3 + 3f_4 \mid^2 \;, \tag{13}$$

$$\left. \frac{d\sigma}{d\Omega} \right|_{\text{mix}} = \tfrac{3}{16} \mid f_1 - f_2 - f_3 + f_4 \mid^2 \;. \tag{14}$$

Equations (13) and (14) give the differential cross sections for the ionic channel and mixed channel, respectively.

For the colliding system $^{16}\text{O} + {}^{28}\text{Si}$ the direct scattering process $^{16}\text{O}(^{28}\text{Si},^{28}\text{Si})^{16}\text{O}$ and 3α transfer process $^{16}\text{O}(^{28}\text{Si},^{16}\text{O})^{28}\text{Si}$ are indistinguishable experimentally. These are in the ionic channel.

The one α transfer reaction process $^{16}\text{O}(^{28}\text{Si},^{24}\text{Mg})^{20}\text{Ne}$ and two α transfer reaction processes $^{16}\text{O}(^{28}\text{Si},^{20}\text{Ne})^{24}\text{Mg}$ are also indistinguishable and these are then in the mixed

TABLE I. Optical potential parameters. $R_i = R_{0i}(A_i^{1/3} + A_2^{1/3})$, $i = V, W, C$.

V_0	V_1	R_{0V}	a_V	W_0	W_1	R_{0W}	a_W	R_{0C}
14.649	0.283	1.363	0.472	−6.001	0.444	1.245	0.497	1.000

channel. In this work calculations have been carried out only for the scattering case.

III. ANALYSIS OF THE POTENTIALS

In this treatment of the 3α exchange mechanism, an additional molecular orbital potential ϵ_μ appears in the total potential of the colliding system, as shown in Eq. (12), $V^{\text{tot}} = V_{\text{I,II}} + \epsilon_\mu$.

In the expression of ϵ_μ in Eq. (9), ϵ is the ground state energy of an α particle bound to the nuclear core. This small constant value can be taken from the experimentally determined value. The direct integral K is the average interaction of a valence particle with one core and it is generally included in the optical potential:

$$V_{\text{I,II}}(R) + 3K(R) = V_{AB}(R) = V^{\text{opt}}(R) + V^{\text{Coul}}(R) \ .$$

An ordinary Woods-Saxon type potential is taken for the optical potential.

Since our calculation covers a certain range of energy, the amplitudes of both real and imaginary potentials are taken to be energy dependent. $V = V_0 + V_1 E$ and $W = W_0 + W_1 E$. The optical potential parameters are listed in Table I.

In the evaluation of the exchange potential in

$$J = \langle \phi_{\text{I}} | v_{\text{II}} | \phi_{\text{II}} \rangle \ , \tag{15}$$

the interaction between an α particle and the nuclear core v_{II} is taken to be the double-Gaussian-type potential,

$$v_i = v_1 e^{-r_i^2/g_1^2} + v_2 e^{-r_i^2/g_2^2}, \quad i = \text{I,II} \ . \tag{16}$$

As the colliding energy increases, the distance between cores, and also the distance from valence particle to core, become closer. The interaction v_i may also change with energy. We have assumed it to be energy dependent: $v_i = v_{i0} + v_{i1}E$, $i = 1,2$. The values chosen for the parameters of the double Gaussian potential are shown in Table II.

As seen in Table II, the coefficients of the energy dependent terms v_{11} and v_{21} in the double Gaussian potential turn out to be small.

In Eq. (15) a wave function of the independent particle model is used for the nuclear orbiting wave function outside ^{16}O,

$$\phi(r) = 8^{-1/2}(\pi a^2)^{-3/4}[(2 - \sqrt{6}) + \sqrt{8/3}(r/a)^2]$$

$$\times \exp(-r^2/2a^2) \ , \tag{17}$$

which has been derived from an α-cluster model of $4N$ nuclei.[22,2] The harmonic oscillator length parameter $a = 1.25$ fm is chosen to give the experimental mean square radius of ^{28}Si. The advantage of applying the independent α particle model and a Gaussian potential is that the exchange potential J can be integrated easily in closed analytic form, as given in the Appendix, although there will exist an inconsistency between Eq. (16) and (17).

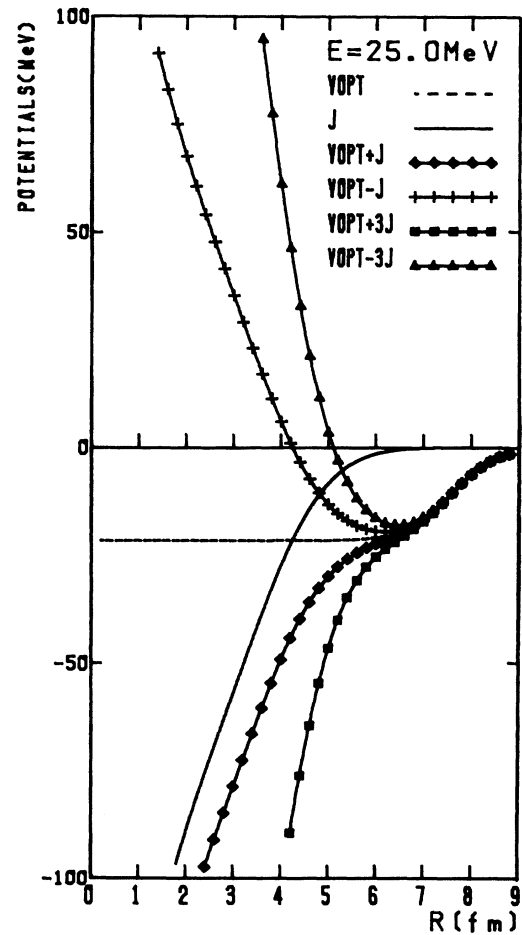If the overlap integral δ is neglected in the expression ϵ_μ

FIG. 3. The combined potentials of the optical and exchange potentials in four possible molecular orbital states. Two of these potentials, $V_{\text{opt}} + J$ and $V_{\text{opt}} + 3J$, are purely attractive, while the other two, $V_{\text{opt}} - J$ and $V_{\text{opt}} - 3J$, show short-range repulsive core and a shallow potential well which provides favorable conditions for forming molecular orbits.
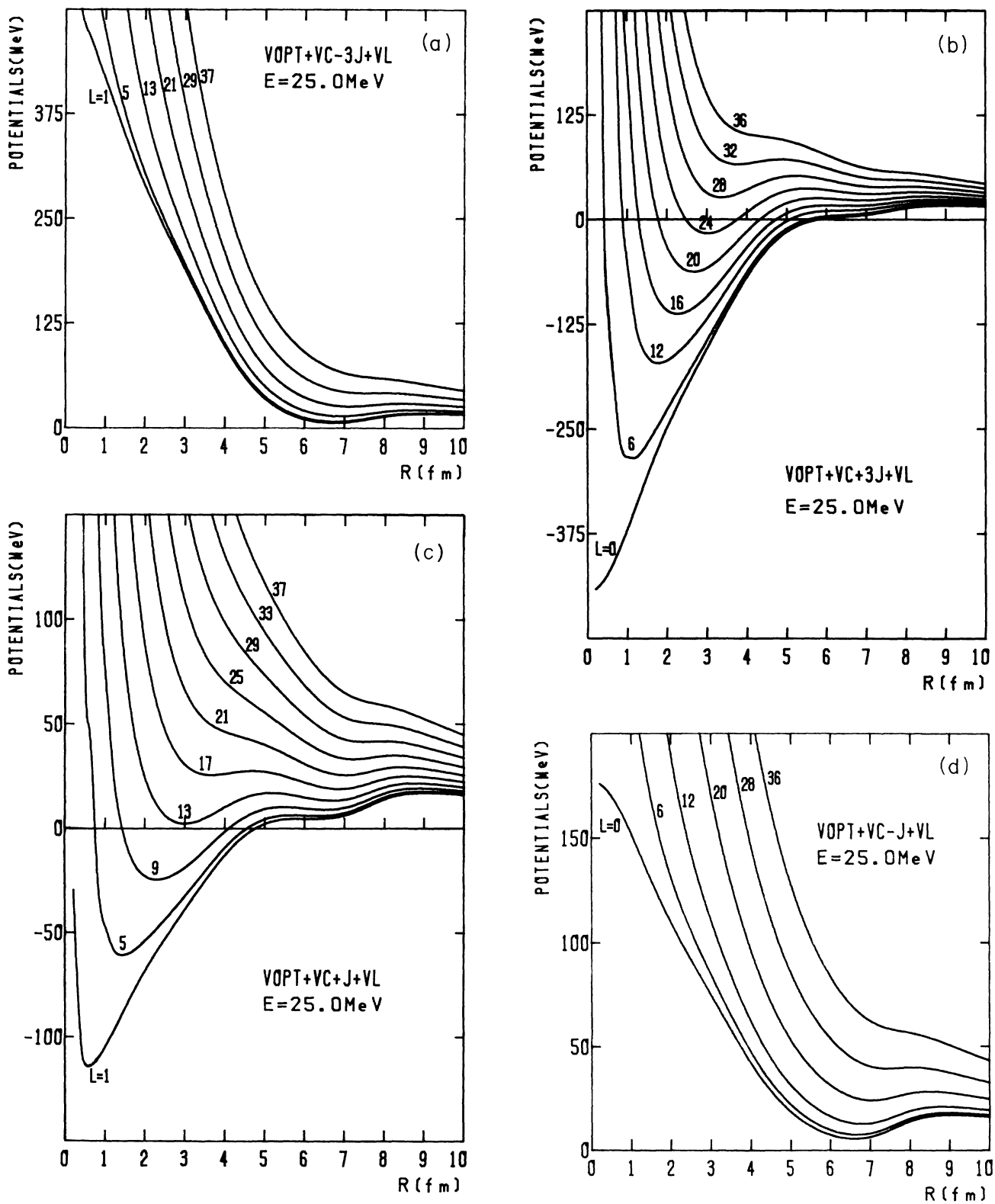
TABLE II. Parameters for the α-^{16}O interaction.

v_{10} (MeV)	v_{11} (MeV)	g_1 (fm)	v_{20} (MeV)	v_{21} (MeV)	g_2 (fm)
711.7	0.117	0.380	−517.3	0.448	3.637

FIG. 4. (a) Total potential of the ^{16}O + ^{28}Si scattering system in a possible molecular orbital state $V_{\text{opt}} + V_C - 3J + V_L$ for odd partial waves $L = 1-37$. Centrifugal potential $V_L = L(L+1)\hbar^2/2mR^2$. (b) Total potential of the ^{16}O + ^{28}Si scattering system in a possible molecular orbital state $V_{\text{opt}} + V_C + 3J + V_L$ for even partial waves $L = 0-36$. (c) Total potential of the ^{16}O + ^{28}Si scattering system in a possible molecular orbital state $V_{\text{opt}} + V_C + J + V_L$ for odd waves $L = 1-37$. (d) Total potential of the ^{16}O + ^{28}Si scattering system in a possible molecular orbital state $V_{\text{opt}} = V_C - J + V_L$ for even partial waves $L = 0-36$.

in Eq. (9), the molecular orbital potential will be $\epsilon_1 \sim -3J$, $\epsilon_2 \sim 3J$, $\epsilon_3 \sim J$, and $\epsilon_4 \sim -J$. ϵ_2, ϵ_3, and the optical potential have the same sign as the $V_{opt} + 3J$ and $V_{opt} + J$ shown in Fig. 3. Nevertheless, ϵ_1 and ϵ_4 have the opposite sign compared with the optical potential. $V_{opt} - 3J$ and $V_{opt} - J$ show repulsive cores and potential wells in the overlapping region. These potential wells should provide the favorite condition for forming molecular states of the colliding system.

If the Coulomb and centrifugal potentials $V(L)$ are also included, the total potential for the four different molecular orbital states, $V_{opt} + V_{Coul} + 3J + V(L)$, $V_{opt} + V_{Coul} - 3J + V(L)$, $V_{opt} + V_{Coul} + J + V(L)$, and $V_{opt} + V_{Coul} - J + V(L)$, are plotted in Fig. 4. As can be seen, in some cases, for certain partial waves, shallow potential wells still exist in the overlapping region.

IV. COMPARISON WITH EXPERIMENT

According to the experimental data available, differential cross sections for the $^{16}O + {}^{28}Si$ scattering system have been calculated in the energy region from $E = 18.67$ to 34.8 MeV. The excitation function at 180° has also been calculated in the energy region for $E = 14-50$ MeV. The theoretical results of differential cross sections are shown in Figs. 2(a)–2(c). Good agreement is reached with the experimental data.[4–6]

The common feature of these angular distributions in Fig. 2 is that in the small angle region the Rutherford scattering dominates, and in the larger angle region nuclear attraction starts to counter the Coulomb effect and makes the experimental curve come down, with some diffraction oscillations. However, after reaching a certain angle the curve starts to rise again, with a more vigorous oscillatory structure.

As we discussed before, the elastic scattering amplitudes come from two contributions, one from direct potential scattering and another from elastic transfer. Direct scattering contributes mainly in the forward angle region, while the elastic transfer scattering contributes mainly in the backward angle region.

If the Coulomb effect were absent, one might expect the experimental curve to be roughly symmetrical about a minimum at 90°. As the incident energy increases, more partial waves with smaller angular momentum are involved in the formation of molecular orbital states, as shown in the analysis of the total potential. The shallow potential well moves into a deeper region and the transfer process is strengthened. The minimum then shifts toward the smaller angle region. Due to the interference and the energy dependent diffraction, more peaks, with narrower widths, appear.

In order to show more clearly the role played by the exchange potential in the angular distribution in the calculation for the $E = 26.2$ MeV case, the exchange potential is deliberately deleted and the optical potential remains. There will be no rising oscillatory structure as shown in Fig. 2(c). The exchange potential appears to play a major role for the rise in the backward angle region.

With the same set of parameters chosen for the angular distributions, the excitation function at 180° has been cal-

culated and plotted as shown in Fig. 1. The number of peaks, their widths, and amplitude all agree fairly well with the experimental curve. The widths of these peaks are mostly on the order of 1–3 MeV. Their lifetime is about the same order of magnitude as the time for the nuclei to travel across the nuclear potential region. It indicates that molecular states are formed only temporarily in the collision process. This may be expected from the existence of shallow potential wells in the overlapping region, as shown in Fig. 4.

The agreement of theoretical and calculations with the number of peaks of the experimental curve may confirm the prediction of the occurrence of four possible molecular orbital states by the theory. The possibility of choosing one common set of parameters to reproduce both the angular distributions and the excitation function encourages us to believe that the 3α transfer mechanism might be a significant process in what is actually happening in the $^{16}O + {}^{28}Si$ scattering.

V. DISCUSSION

When two nuclei approach each other and start to overlap, all the nucleons will interact with each other. Depending on the incident energy, these nucleons may undergo excitation, regrouping, transfer, or may form a compound nucleus and break up. Of course, these two colliding nuclei may also maintain their internal structure while being elastically scattered. In this case a one-particle optical potential is then assumed to describe the elastic scattering. However, in a rather wide energy region the collision between two heavy ions can generally proceed in many different ways. The substitution of this many-body problem of a system with two $4N$ nuclei by a one-particle optical potential may be too strong an assumption.

For this scattering system of ^{16}O with ^{28}Si, we have assumed 3α exchange to be the main process in the transfer mechanism. If the nuclear cores are identical, one will get the desired parity dependent exchange potential to interpret the anomalous phenomena observed. A process with 12 nucleons exchanged between two identical ^{16}O cores is then more likely expected to occur. Since the α particle has the highest binding energy, an α cluster should have a greater probability of being formed and transferred in the overlapping region than other kinds of clusters.

The possibility of the formation and transfer of a ^{12}C cluster in the scattering process may also be small. In our previous study of the scattering system $^{16}O + {}^{24}Mg$, calculations were performed for two cases: transfer of one ^{8}Be cluster and two-α-cluster transfer. It was found that, for fitting the experimental data, an unreasonably large value is needed for the spectroscopic factor for the case of ^{8}Be transfer, while for the 2α transfer case the adjusted value agrees with the experimental spectroscopic factor.

In order to interpret the large number of peaks observed in the excitation function of the scattering system $^{12}C + {}^{12}C$, Michaud and Vogt noted that with a two-body Imanishi approach there was no way of obtaining this large number of resonances while retaining any reasonable potential well radius.[23] They have already proposed a

mechanism wherein the resonances correspond to intermediate cluster states of three alpha particles moving relative to the remaining ^{12}C core. By introducing additional degrees of freedom in the form of these three alpha particle clusters about an assumed undisturbed ^{12}C core, they were able to accommodate the increased number of resonances. The ^{12}C nucleus breaks up during the collision process.

In this treatment the recoil of the cores has been neglected. This appears to be very serious when the transfer of three α clusters between cores of mass 16 is considered. However, for a three-particle system formed by two identical cores plus one valence particle, Fonseca and Shanley made a systematic investigation and found that the Born-Oppenheimer approximation yields remarkably good results for the binding energies and wave functions, even when the mass ratio of core to valence particles is not large $(M/m \geq 1)$.[24] In LCNO theory the 3 α particles are supposed to be transferred through the formation of molecular orbits around the cores. The recoil effect caused by the transfer of three alpha particles this way might not be as serious as that caused by a direct 3α transfer process in a distorted-wave Born-approximation treatment.

The potential between heavy ions has been one of the most challenging and well investigated problems in nuclear physics. Many microscopic models based on approximations to the many-particle Schrödinger equation with the consideration of the exclusion principle have been established, such as the resonating group model, generator coordinates method, etc. Due to the difficulties of solving the many-body problem, no exact solutions could be expected, although some behavior of the heavy-ion potential may be predicted.

The α-cluster model reduces the many-body problem to a few-body problem. In particular, due to the spinless nature of both the valence particles and the nuclear cores the treatment becomes most simple to handle analytically. It can be seen clearly how a strong repulsive core is created by the consideration of symmetrical exchange properties of the identical cores and identical valence particles in the exchange potential. This gives a strong resistance for preventing the interpenetration of the two colliding nuclei. It also shows how a shallow potential well is formed in the overlapping of the two nuclei by the consideration of both the optical potential between the cores and the interaction between valence particles and the cores.

In order to attain physical insight into the problem, the treatment is kept as simple as possible. Improvements, of course, can be made in many ways.

APPENDIX

An exact expression of the exchange potential can be obtained in closed form by using an independent α model wave function and a double Gaussian potential for the α-core interaction. The independent α model wave function is written as

$$\phi_i = (A_1 + A_2 r_i^2)e^{-\alpha r_i^2}, \quad i = \text{I,II}$$

with $A_1 = -0.067\,346\,09a^{-3/2}$, $A_2 = 0.244\,667\,88a^{-7/2}$, and $\alpha = 0.5a^{-2}$. The double Gaussian potential is

$$v_i = v_1 e^{-\lambda_1 r_i^2} + v_2 e^{-\lambda_2 r_i^2}, \quad i = \text{I,II}$$

with $\lambda_1 = 1/g_1^2$ and $\lambda_2 = 1/g_2^2$.

The exchange potential can then be integrated easily as

$$J = \langle \phi_I | v_{II} | \phi_{II} \rangle$$
$$= \sum_{i=1}^{2} \sum_{k=1}^{2} \sum_{j=1}^{2} A_i v_k A_j I_{ij}(\alpha, \lambda_k + \alpha) ,$$

where

$$I_{11}(\alpha,\beta) = \left[\frac{\pi}{\alpha + \beta} \right]^{3/2} e^{-[\alpha\beta/(\alpha+\beta)]R^2} ,$$

$$I_{12}(\alpha,\beta) = \frac{1}{\alpha+\beta} \left[\frac{3}{2} + \frac{\alpha^2}{\alpha+\beta} R^2 \right] I_{11}(\alpha,\beta) ,$$

$$I_{21}(\alpha,\beta) = I_{12}(\beta,\alpha) ,$$

$$I_{22}(\alpha,\beta) = \frac{1}{(\alpha+\beta)^2} \left[\frac{15}{4} + \frac{2(\alpha-\beta)^2 + \alpha^2 + \beta^2}{2(\alpha+\beta)} R^2 \right.$$
$$\left. + \left[\frac{\alpha\beta}{\alpha+\beta} \right]^2 R^4 \right] I_{11}(\alpha,\beta) .$$

[1]W. von Oertzen and H. G. Bohlon, Phys. Rep. 19c, 1 (1975).

[2]Guozhu He, Chengqun Gao, and Pingzhi Ning, Phys. Rev. C 30, 534 (1984).

[3]Chengqun Gao, Pingzhi Ning, and Guozhu He, Nucl. Phys. A438, 281 (1985).

[4]P. Braun-Munzinger, G. M. Berkowitz, T. M. Cormier, C. M. Jachcinski, J. W. Harris, J. Barrette, and M. J. LeVine, Phys. Rev. Lett. 38, 944 (1977).

[5]C. K. Gelbke, T. Awes, U. E. P. Berg, J. Barrette, M. J. LeVine, and P. Braun-Munzinger, Phys. Rev. Lett. 41, 1778 (1978).

[6]P. Braun-Munzinger, G. M. Berkowitz, M. Gai, C. M. Jachcinski, T. R. Renner, C. D. Uhlhorn, J. Barrette, and M. J. LeVine, Phys. Rev. C 24, 1010 (1981).

[7]S. Kahana, J. Barrette, B. Berthier, E. Chavez. A Greiner, and M. C. Mermaz, Phys. Rev. C 28, 1393 (1983).

[8]M. C. Mermaz, E. R. Chavez-Lomeli, J. Barrette, B. Berthier, and A. Greiner, Phys. Rev. C 29, 147 (1984).

[9]P. Braun-Munzinger and J. Barrette, Phys. Rep. 87, 209 (1982).

[10]V. Shkolnik, D. Denhard, S. Kuboni, M. A. Franey, and S. Tripp, Phys. Lett. 74B, 195 (1978).

[11]S. Kahana, G. Pollarolo, J. Barrette, A. Winther, and R.

Brogha, Phys. Lett. **133B**, 283 (1983).

[12]A. M. Kobos, G. R. Satchler, and R. S. Mackintosh, Nucl. Phys. **A395**, 248 (1983).

[13]A. M. Kobos and G. R. Satchler, Nucl. Phys. **A427**, 589 (1984).

[14]L. F. Canto, R. Donangelo, M. S. Hussein, and A. Lepine-Szily, Phys. Rev. Lett. **51**, 95 (1983).

[15]G. R. Satchler and W. G. Love, Phys. Rep. **55**, 183 (1979).

[16]J. Barrette and S. Kahana, Comments Nucl. Part. Phys. **9**, 67 (1980).

[17]R. S. Mackintosh and A. M. Kobos, Phys. Lett. **92B**, 59 (1980).

[18]K. A. Gridnev and A. A. Ogloblin, Fiz. Elem. Chastits At. Yadra **6**, 393 (1975) [Sov. J. Part. Nucl. **6**, 393 (1975)].

[19]V. N. Bragin, Yad. Fiz. **36**, 656 (1982) [Sov. J. Nucl. Phys. **36**, 387 (1982)].

[20]A. I. Baz, V. Z. Goldberg, K. A. Gridnev, V. M. Semjonov, and E. F. Hefter, Z. Phys. A **280**, 171 (1977).

[21]V. N. Bragin and R. Donangelo, Nucl. Phys. **A433**, 495 (1985).

[22]Q. R. Li, S. Z. Chen, and E. G. Zhao, Phys. Ener. Fort. Phys. Nucl. (China) **5**, 531 (1981).

[23]G. Michaud and E. W. Vogt, Phys. Lett. **30B**, 85 (1969); Phys. Rev. C **5**, 350 (1972).

[24]A. C. Fonseca and P. E. Shanley, Ann. Phys. (N.Y.) **117**, 268 (1979).